·临床研究·

磁共振成像卵巢-附件影像报告和数据系统鉴别良恶性病变应用价值

伏文皓，胡笑笑，孙梦雅，张　繁，王　珂，唐广磊，关　键
(中山大学附属第一医院医学影像科，广东 广州 510080)

摘　要：【目的】探讨磁共振成像卵巢-附件影像报告和数据系统(O-RADS MRI)在鉴别卵巢-附件良性和恶性病变上的应用价值。【方法】回顾性收集2020年1月至2022年2月中山大学附属第一医院经手术病理证实的146例卵巢-附件病变成年患者(共202个肿块)，所有患者均按O-RADS MRI标准扫描方案行3.0 T MR盆腔检查。由两名放射科医生根据O-RADS MRI对卵巢-附件肿块进行1~5评分，运用Cohen's kappa检验评估2名医生评分结果的一致性。以手术病理结果为金标准，计算O-RADS MRI各评分恶性肿块的检出率。以O-RADS MRI 3分为诊断界值，计算O-RADS MRI诊断恶性卵巢-附件肿块的敏感度、特异度、准确度和曲线下面积。【结果】202个卵巢-附件肿块中，恶性肿块62个(30.7%)，良性肿块140个(69.3%)。采用O-RADS MRI评估时2名医生间的Cohen's Kappa系数为0.932。O-RADS MRI 1-5分卵巢-附件肿块恶性率分别为：0%，0%，7.7%，95%，97.6%。O-RADS MRI诊断恶性卵巢-附件肿块的敏感度、特异度、准确度、曲线下面积分别为96.8%(60/62)、98.6%(138/140)、98.0%(198/202)、0.977。【结论】O-RADS MRI对区分卵巢-附件良恶性肿块有极佳的诊断效能，且该标准化报告系统的广泛实施可改善放射科医生和临床医生之间的沟通，优化卵巢-附件肿块患者的管理，值得临床推广应用。

关键词：磁共振成像；卵巢-附件影像报告和数据系统；卵巢-附件肿块；临床应用
中图分类号：R445.2　　**文献标志码**：A　　**文章编号**：1672-3554(2023)01-0099-07
DOI：10.13471/j.cnki.j.sun.yat-sen.univ(med.sci).20221201.002

Value of MRI Ovarian-Adnexal Reporting and Data System in Differentiating Benign and Malignant Ovarian-Adnexal Lesions

FU Wen-hao, HU Xiao-xiao, SUN Meng-ya, ZHANG Fan, WANG Ke, TANG Guang-lei, GUAN Jian
(Department of Medical Imaging, The First Affiliated Hospital, Sun Yat-sen University, Guangzhou 510080, China)
Correspondence to: GUAN Jian; E-mail: guanj6@mail.sysu.edu.cn

Abstract: 【Objective】 To explore the value of MRI ovarian-adnexal reporting and data system (O-RADS MRI) in differentiating benign and malignant ovarian-adnexal masses. 【Methods】 Totally 146 patients (202 masses) with ovarian-adnexal lesions who underwent pelvic examination at 3.0 T MRI according to standardized scan protocol of O-RADS MRI and were pathologically confirmed in The First Affiliated Hospital of Sun Yat-sen University between January 2020 and February 2022 were retrospectively analyzed. Two radiologists classified the ovarian-adnexal masses as risk levels 1~5 according to O-RADS MRI and evaluated their consistency by Cohen's kappa. Using pathological findings as the gold standard, the detection yield of malignant lesions with O-RADS MRI classification was analyzed. Sensitivity, specificity, accuracy, and the area under the receiver operating characteristic curve were calculated (cutoff for malignancy, score ≥ 4). 【Results】 Of 202 masses, 62 (30.7%) were malignant, 140 (69.3%) were benign. The two radiologists presented good

收稿日期：2022-10-12
基金项目：国家自然科学基金(82273242)
作者简介：伏文皓，学士，研究方向：生殖泌尿系统影像，E-mail：fuwh6@mail.sysu.edu.cn；关键，通信作者，E-mail：guanj6@mail.sysu.edu.cn

agreement in O-RADS MRI classification of ovarian adnexal masses (Kappa=0.932). The malignancy rates of masses with scores of 1, 2, 3, 4 and 5 were 0%, 0%, 7.7%, 95%, 97.6%, respectively. Sensitivity, specificity, accuracy, and the area under the receiver operating characteristic curve were 96.8% (60/62), 98.6% (138/140), 98.0% (198/202), 0.977. 【Conclusions】O-RADS MRI yields high diagnostic efficiency for benign and malignant ovarian adnexal masses and its widespread implementation will improve communication between radiologists and clinicians, and facilitate optimal patient management. Therefore, O-RADS MRI warrants widespread use in clinical setting.

Key words: magnetic resonance imaging; ovarian-adnexal reporting and data system; ovarian-adnexal masses; clinical practice

[J SUN Yat-sen Univ(Med Sci),2023,44(1):99-105]

超声是无创性检测并初步评估卵巢-附件肿块的一线工具[1]。超声可以将大多数卵巢-附件肿块准确划分为良性或恶性,但仍有18%~31%卵巢-附件肿块的诊断不能明确[2-3]。在鉴别卵巢-附件良恶性肿块方面,磁共振成像(magnetic resonance imaging, MRI)已被证实比其他成像方式具有更高的准确性[4-5]。2022年,美国放射学会(American college of radiology,ACR)正式发布了卵巢-附件影像报告和数据系统(ovarian-adnexal reporting and data system,O-RADS)磁共振成像风险分层系统(O-RADS MRI)的指南[6]。该指南是ACR磁共振工作小组在2013年发表的ADNEX MR评分系统[7]的基础上推出的,是卵巢-附件肿块恶性概率的风险分层系统,其主要目标是基于标准化影像数据来改善放射科医生和临床医生之间的沟通,优化卵巢-附件病变患者的治疗。本研究的目的是探讨O-RADS MRI在鉴别卵巢-附件良性和恶性病变上的应用价值。

1 材料与方法

1.1 研究对象

本研究已通过中山大学附属第一医院医学伦理委员会批准,因属回顾性研究免除签署病人知情同意书。回顾性收集2020年1月至2022年2月于中山大学附属第一医院就诊的卵巢-附件病变患者,所有患者均行手术治疗并有病理诊断结果。纳入标准:①年龄>18岁;②既往无子宫及双卵巢-附件全切手术史。排除标准:①未按O-RADS MRI标准扫描方案行3.0 T盆腔MR检查;②病理结果不明确。最终入组146例患者,年龄18~87岁,中位年龄41岁;绝经前103例,绝经后43例。

1.2 MR检查及图像后处理

所有患者均使用Siemens Magnetom Trio 3.0 T MR扫描仪和8通道相控阵盆腔线圈获取MR图像。患者取仰卧位,扫描范围自下腹髂嵴水平到盆底耻骨联合水平。采集的序列如下:矢状位非脂肪抑制T_2WI;轴位非脂肪抑制T_2WI;轴位非脂肪抑制T_1WI及T_1 Dixon;轴位DWI;轴位脂肪抑制T_1WI动态增强(dynamic contrast enhanced, DCE)成像。对比剂为钆特酸葡胺(江苏恒瑞医药股份有限公司,含钆特酸葡胺377 mg/mL),经肘静脉以流率2 mL/s注入0.2 mL/kg的剂量,推注对比剂前30 s开始扫描以获取非增强图像用于减影,推注对比剂后进行连续无间断扫描获取DCE图像(时间间隔0 s;总时间至少4 min;时间分辨率15 s)。扫描参数详见表1。

绘制DCE图像时间-信号强度曲线(time-intensity curve, TIC)的方法如下:所有图像都发送到Syngo.via工作站,根据O-RADS MRI标准化词典的建议[8],在病变实性组织中最早开始强化的部分及子宫外肌层(应避开子宫肌层的血管或病变,如子宫平滑肌瘤或子宫腺肌症)分别勾画感兴趣区(region of interest, ROI),通过灌注工具自动获取DCE TIC。

1.3 图像分析及分组

由2名至少有10年磁共振诊断经验的放射科医生经O-RADS MRI培训后,以O-RADS MRI词典为依据,采用双盲法独立按照O-RADS MRI风险分层指南对每个病变进行评分,并达成一致意见[6,8-9]。重点评估内容为病变的最大径(重复三次测量取平均值)、单侧或双侧、病变类型(囊性、囊实性或实性,T_2WI和高b值DWI都呈均匀双低信号的病变,简称"双低"病变)及组成(囊内容物成分)和实性组织的增强模式(即DCE TIC类型,分为低风险型、中风险型、高风险型)、转移征象(腹膜结节或不规则增厚、淋巴结转移、骨转移等)[9]。将O-RADS MRI评分进行二分类,1~3分为良性,4~5分为恶性[10]。以手术病理结果为金标准,分为良性病变和恶性病变,后者包括交界性肿瘤和侵袭性肿瘤。

1.4 统计分析

采用SPSS 25.0和MedCalc15.2.2软件进行统计学分析。计量资料以($\bar{x} \pm s$)表示,计数资料以率(%)表示。采用Cohen's kappa评估2名放射科医生评分结果的一致性。分别计算O-RADS MRI 1~5分卵巢-附件恶性病变的检出率(阳性预测价值)。以O-RADS MRI 3分为诊断界值,计算O-RADS MRI诊断恶性卵巢-附件病变的敏感度、特异度、准确度,并采用受试者工作特性曲线(receiver operating characteristic, ROC)评估诊断价值。采用Kolmogorov-Smirnov检验进行正态分布检验,Bartlett's检验进行方差齐性检验后,根据变量类型合理采用两独立样本t检验和χ^2检验或Fisher精确检验进行良、恶性卵巢-附件病变MRI征象的比较。$P<0.05$为差异有统计学意义。

表1　O-RADS MRI扫描序列及参数

Table 1　MR scanning sequences and parameters

Items	T_2WI	T_2WI	T_1WI	DWI	DCE
Orientation	Sagittal	Axial	Axial	Axial	Axial
Sequence	Fast Spin echo	Fast Spin echo	Fast Spin echo	Single-shot EPI	Gradient echo
TR/msec	5 900	5 900	450	7 560	2.90
TE/msec	101	101	9.2	64	1.18
Flip angle /degree	120	120	120	90	12.5
FOV/mm	250 × 250	230 × 230	230 × 230	280 × 267	250 × 201
Matrix	288 × 384	288 × 384	269 × 384	128 × 134	209 × 288
Slice thickness /mm	4	3	3	3	3
Slice gap/mm	0.4	0.3	0.3	0.3	0.3
Number of excitations	2	2	2	–	2
Echo train length	12	12	77	–	–
B values	–	–	–	0，1 000 s/mm^2	–

2　结果

本研究入组146例患者，患者年龄符合正态分布，具有方差齐性，为18~87（44±13）岁。95例患者有1个病灶，46例有2个病灶，5例有3个病灶，共202个病灶，其中127个为卵巢起源，19个为输卵管起源。恶性肿块有62个（30.7%），良性肿块有140个（69.3%）（表2）。O-RADS MRI 1~5分各有21个，93个，26个，20个，42个（表3，图1~图5）。O-RADS MRI 1~5分卵巢-附件肿块恶性率分别为0%，0%，7.7%，95%，97.6%。O-RADS MRI诊断恶性卵巢-附件肿块的敏感度、特异度、准确度分别为96.8%（60/62）、98.6%（138/140）、98.0%（198/202）。曲线下面积ROC Area，AUROC（95% CI）0.977（0.949，1.000）。采用O-RADS MRI评分时，两名放射科医生的kappa（95% CI）0.932（0.879，0.985），P <0.001，具有很好的一致性。

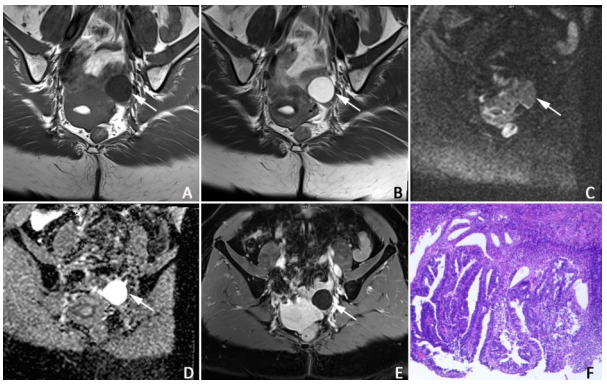

A 45-year-old female with left ovarian simple cyst. The cyst (<3 cm) showed hypointensity on coronal T1-weighted image (A), hyperintensity on coronal T2-weighted image (B), hypointensity on high B-value DWI (C) and hyperintensity on ADC map (D) with no enhancement on coronal post-contrast fat-suppressed T1WI (E). F: Microscopy in hematoxylin and eosin.

图1　O-RADS MRI 1分

Fig. 1　O-RADS MRI score 1

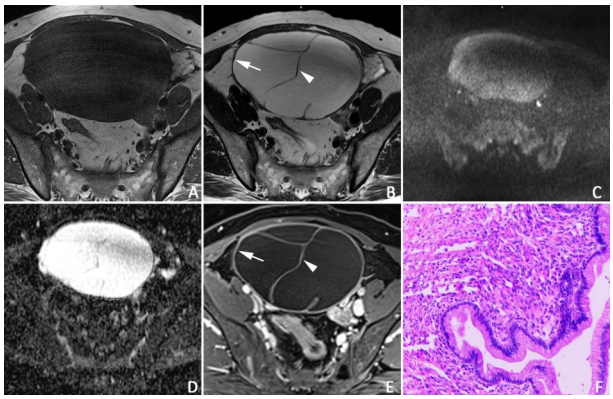

A 51-year-old female with right mucinous cystadenoma. The multilocular cystic mass showed hypointensity on axial T1-weighted image (A), hyperintensity on axial T2-weighted image (B), hyperintensity on high B-value DWI (C) and ADC map (D) with enhanced smooth wall (arrow) and septation (arrowhead) of the mass on axial post-contrast fat-suppressed T1WI (E). F: Microscopy in hematoxylin and eosin.

图3　O-RADS MRI 3分

Fig. 3　O-RADS MRI score 3

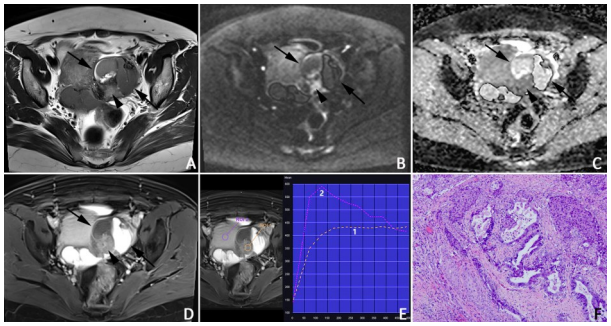

A 40-year-old female with left mucinous endometrioid borderline tumor and endometrioma. The solid tissue (arrowhead) of the mass showed isointensity on axial T2-weighted image (A), hyperintensity on high B-value DWI (B) and hypointensity on ADC map (C) with homogeneous enhancement on axial post-contrast fat-suppressed T1WI (D). E: The intermediate-risk TIC showed a moderate initial rise in the signal intensity of solid tissue, with a slope slower than that of the myometrium, with a shoulder and plateau (1 refer to the curve of the mass and 2 refer to that of the myometrium). F: Microscopy in hematoxylin and eosin.

图4 O-RADS MRI 4分

Fig. 4 O-RADS MRI score 4

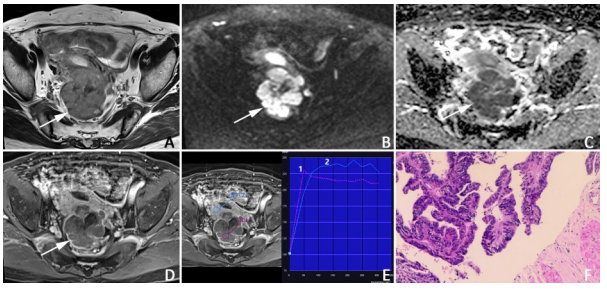

A 70-year-old female with left high-grade serous carcinoma. The solid mass showed isointensity on axial T2-weighted image (A), hyperintensity on high B-value DWI (B) and hypointensity on ADC map (C) with inhomogeneous enhancement on axial post-contrast fat-suppressed T1WI (D). E: The high-risk TIC showed a brisk initial rise in the signal intensity of solid tissue, with a slope greater than myometrium, with a shoulder and plateau. (1 refer to the curve of the mass and 2 refer to that of the myometrium). F: Microscopy in hematoxylin and eosin.

图5 O-RADS MRI 5分

Fig. 5 O-RADS MRI score 5

卵巢-附件良、恶性病变的MRI征象比较见表4。双侧发病的情况($P = 0.966$)、病变的最大径($P = 0.400$)和中风险型曲线($P = 0.052$)对于鉴别良恶性无确切帮助,此外纯脂肪性病变由于例数过少,也不能明确其诊断价值($P = 1.000$)。118个囊性病变都是良性,纯粹的囊性肿物是良性病变的典型特征($P < 0.001$)。部分卵巢-附件良性病变可表现为囊实性,实性部分表现为以下四种情况不规则分隔、壁结节、乳头状突起、肿块,都提示恶性病变可能性大($P < 0.05$)。

表2 202个卵巢-附件病变的病理结果

Table 2 Pathologic findings of 202 ovarian-adnexal lesions

Pathologic findings			202
Benign	140	Borderline and invasive	62
Serous cystadenoma	3	Serous borderline tumor	5
Mucinous cystadenoma	9	Mucinous borderline tumor	7
cystadenoma	1	Endometrioid borderline tumor	2
Mature cystic teratoma	8	Granulosa cell tumor	1
Thecoma / Fibroma	1	Serous carcinoma	20
Thecofibroma	4	Mucinous carcinoma	3
Fibroma	2	Endometrioid carcinoma	5
Mixed germ cell-sex cord stromal tumor	1	Clear cell carcinoma	3
Myoma	1	Yolk sac tumor	3
Endometrioma	67	Mixed germ cell tumor	1
Other[1)]	43	Metastasis and lymphoma	12

[1)] Benign cyst, hydrosalpinx, foreign body granuloma, hemorrhagic cyst, tubo-ovarian abscess.

良、恶性卵巢-附件病变均可表现为实性肿块。在10例(11个)表现为实性肿块的良性病变中,其中8个为双低病变,3个病变时间-信号强度曲线呈低风险型。在21例(23个)表现为实性肿块的恶性病变中,5个病变曲线呈中

表3　O-RADS MRI对卵巢-附件病变评估的结果

Table 3　O-RADS MRI classification of ovarian adnexal masses

O-RADS MRI Score	Total(*N*=202)	Benign(*n*=140)	Malignant (*n*=62)		Malignancy rate/%
			Borderline(*n*=15)	Invasive(*n*=47)	
1	21	21 (15.0)	0	0	0
2	93	93 (66.4)	0	0	0
3	26	24 (17.1)	2 (13.3)	0	7.7
4	20	1 (0.7)	13 (86.7)	6 (12.8)	95.0
5	42	1 (0.7)	0	41 (82.2)	97.6

Data are numbers of lesions, with percentages in parentheses.

表4　良、恶性卵巢-附件病变MRI征象比较

Table 4　Comparison of MR Imaging Parameters between Benign and Malignant Tumors

MRI Imaging Parameter	Benign (*n*=140)	Malignant (*n*=62)	χ^2/t	*P*
Size/mm[1)]	65.57 ± 46.51	82.05 ± 45.14	−2.075	0.400[2)]
Bilaterality	22.86 (32/140)	22.58 (14/62)	0.002	0.966
Cystic(without solid tisse)	84.29 (118/140)	0	125.666	< 0.001
Simple fluid	38.57 (54/140)	0	32.64	< 0.001
Endometriotic fluid	44.29 (62/140)	0	49.693	< 0.001
Fat- or -lipid-containing fluid	1.43 (2/140)	0	0.001	1.000
Cystic and solid (with solid tissue)	7.86 (11/140)	62.90 (39/62)	69.905	< 0.001
Papillary projection	0	4.84 (3/62)	6.876	0.028
Irregular septation / wall	5 (7/140)	14.52 (9/62)	4.743	0.044
Mural nodule	2.86 (4/140)	25.81 (16/62)	20.594	< 0.001
Larger solid portion	0	17.74 (11/62)	26.269	< 0.001
Solid (with solid tissue)	7.86 (11/140)	37.10 (23/62)	26.244	< 0.001
T2 dark/ DWI dark[3)]	36.36 (8/22)	0	24.919	< 0.001
TIC				
Low risk TIC	85.71 (12/14)	0	63.107	< 0.001
Intermediate risk TIC	7.14 (1/14)	37.10 (23/62)	4.743	0.052
High risk TIC	7.15 (1/14)	62.90 (39/62)	13.162	< 0.001
Peritoneal thickening, nodule	0	33.87 (21/62)	52.921	< 0.000
Other Metastasis (*e.g.*, lymph node and bone metastasis)	0	6.45 (4/62)	9.215	0.008

Unless otherwise stated, data are percentages, with raw data in parentheses. [1)] Data are means ± standard deviations. [2)] Calculated with the student's *t*-test; all other *P* values were calculated by using the chi-square test. [3)] Low T2-weighted and low b = 1 000 sec/mm^2 - weighted signal intensity within solid tissue.

风险型、18个病变曲线呈高风险型，其中17例可见转移(14例腹膜转移、2例淋巴结转移和骨转移、1例淋巴结转移)。双低病变和低风险型曲线都是良性病变的可靠征象($P < 0.001$)，而高风险型曲线($P < 0.001$)和图像上的任何转移征象($P < 0.05$)是恶性病变的可靠征象。

3　讨 论

3.1　O-RADS MRI的背景

准确识别卵巢-附件肿块对于优化患者管理至关重要。

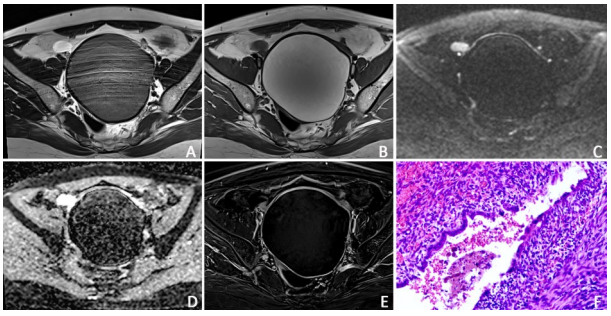

A 37-year-old female with right endometrioma. The cyst (>3 cm) showed hyperintensity on axial T1-weighted image (A), hypointensity on axial T2-weighted image (B), hypointensity on high B-value DWI (C) and ADC map (D) with enhanced smooth wall of the cyst on the subtracted image of post-contrast T1WI (E). F: Microscopy in hematoxylin and eosin.

图2 O-RADS MRI 2分

Fig. 2 O-RADS MRI score 2

尽管超声检查可将大多数卵巢-附件肿块准确划分为良性或恶性,但在使用超声国际卵巢肿瘤分析(international ovarian tumor analysis, IOTA)或超声O-RADS风险分层系统评估后,18%-31%卵巢-附件肿块的诊断仍不能明确[2-3]。当卵巢-附件肿块在超声上诊断不明确时,恶性肿瘤的阳性预测值为7%到50%[11-12],MRI能将此类病变的阳性预测值增加到71%,同时阴性预测值为98%[10]。MRI能够为超声诊断不明确的病变(18%~31%)提供更具体的诊断,从而改善恶性病变的预后并降低良性病变的手术率[13-15]。

3.2 O-RADS MRI对卵巢-附件肿块的诊断效能

目前,已经有多项研究验证了O-RADS MRI对良性和恶性卵巢-附件肿块的诊断效能很高(85.6%-99% 敏感度,78%-97.5% 特异度)[4, 10]。此外,先前用于鉴别卵巢-附件良恶性的评分系统为ADNEX MRI,其敏感度为85.6%-93.5%,特异度为84.6%-97.5%[1, 16-18]。本研究中,O-RADS MRI鉴别良性和恶性卵巢-附件肿块具有极高的敏感度、特异度和准确度(分别为96.1%、98.2%和97.5%),曲线下面积ROC Area, AUROC (95% CI) = 0.977 (0.949, 1.000),这与之前对该评分系统及ADNEX MRI的验证试验结果相似[1, 4, 10, 16-18]。本研究中,O-RADS MRI 1分,2分,3分,4分,5分卵巢-附件肿块恶性率分别为0%,0%,7.7%,95%,97.6%。Thomassin-Naggara等报道的O-RADS MRI 1分,2分,3分,4分,5分卵巢-附件肿块恶性率分别为10.9%,0.3%,5.6%,55.5%,89.5%[10],其中1分和4分卵巢-附件肿块的恶性率有差异,原因可能为本研究中卵巢-附件肿块数量少,这需要大样本量和多中心的研究来证实。

3.3 本研究一致性分析及误诊分析

两名放射科医生的O-RADS MRI评分判定一致性极好, kappa(95% CI)= 0.932(0.879,0.985),P <0.001。两名医生在各自评估后,202个病灶中仅有6个病灶存在分歧,但最终经讨论达成了一致。两名医生对4个多房囊性肿块的分隔是光滑还是不规则存在分歧,后经讨论确定为光滑分隔而判为O-RADS MRI 3分,病理结果4例均为卵巢黏液性囊腺瘤。分隔光滑还是不规则属主观判断也是评判的难点,需要放射科医生在实践中积累经验,并在O-RADS MRI评分中予以重视[19]。此外,两名医生对2个实性肿块是否为双低病变存在分歧,一名医生认为是双低病变而判为O-RADS MRI 2分,而另一名医生则认为病灶内存在小片状T_2WI高信号而不属于双低病变,并根据病变的高风险TIC判为5分,后经讨论该实性肿块绝大部分都呈均匀T_2WI和高b值DWI低信号(小片状T_2WI高信号属于囊变)应被判为双低病变,评分为2分,病理结果为卵巢卵泡膜纤维瘤。除颗粒细胞瘤外,卵巢性索间质肿瘤大多数表现为实性肿块,T_2WI为低信号,但病变较大(>6 cm)时可出现囊性变,在O-RADS MRI评分中应酌情考虑[20]。

本研究中共有以下4例误诊病例,2例卵巢交界性黏液性囊腺瘤被评为3分,原因为病灶内的不规则分隔未被识别,这需要在诊断前得到充分地训练并严格遵守O-RADS MRI评分规则[21]。1例慢性化脓性输卵管炎被评为4分,是因为将因慢性炎症而增厚的输卵管壁或输卵管内皱襞误判为实性组织,应结合其他特征协助诊断,例如管状结构、邻近结构炎性改变等[21]。1例良性的卵巢子宫内膜异位症被评为5分,原因为对病变内的壁结节进行了曲线分析,结果为高风险TIC而被误判为O-RADS MRI 5分。除了表现为纯囊性病灶的巧克力囊肿外,部分子宫内膜异位症也可有增强的壁结节[22-23]。伴有实性组织的子宫内膜异位症的诊断对O-RADS MRI具有挑战性。

3.4 本研究的局限性

本研究的局限性在于:第一,本研究为单中心研究,无法反映其他机构MRI检查的情况。第二,本研究未纳入年龄小于18岁的患者。第三,本研究为回顾性研究,并没有将O-RADS MRI应用于临床管理,因此该系统对患者治疗和预后的影响是未知的。

总的来说,O-RADS MRI对区分卵巢-附件良恶性肿块有极佳的诊断效能,且该标准化报告系统的广泛实施可改善放射科医生和临床医生之间的沟通,优化卵巢-附件肿块患者的管理,值得临床推广应用。

参考文献

[1] Basha MAA, Abdelrahman HM, Metwally MI, et al. Validity and Reproducibility of the ADNEX MR scoring system in the diagnosis of sonographically indeterminate adnexal masses [J]. J Magn Reson Imaging, 2021, 53(1): 292-304.

[2] Froyman W, Landolfo C, De Cock B, et al. Risk of

complications in patients with conservatively managed ovarian tumours (IOTA5): a 2-year interim analysis of a multicentre, prospective, cohort study [J]. Lancet Oncol, 2019, 20(3): 448-458.
[3] Andreotti RF, Timmerman D, Strachowski LM, et al. O-RADS US risk stratification and management system: a consensus guideline from the ACR ovarian-adnexal reporting and data system committee[J]. Radiology, 2020, 294(1): 168-185.
[4] Aslan S, Tosun SA. Diagnostic accuracy and validity of the O-RADS MRI score based on a simplified MRI protocol: a single tertiary center retrospective study [J]. Acta Radiol, 2021: 2841851211060413.
[5] Thomassin-Naggara I, Toussaint I, Perrot N, et al. Characterization of complex adnexal masses: value of adding perfusion- and diffusion-weighted MR imaging to conventional MR imaging[J]. Radiology, 2011, 258(3): 793-803.
[6] Sadowski EA, Thomassin-Naggara I, Rockall A, et al. O-RADS MRI Risk Stratification System: Guide for assessing adnexal lesions from the ACR O-RADS committee[J]. Radiology, 2022, 303(1): 35-47.
[7] Thomassin-Naggara I, Aubert E, Rockall A, et al. Adnexal masses: development and preliminary validation of an MR imaging scoring system [J]. Radiology, 2013, 267(2): 432-443.
[8] Reinhold C, Rockall A, Sadowski EA, et al. Ovarian-adnexal reporting lexicon for MRI: a white paper of the acr ovarian-adnexal reporting and data systems MRI committee [J]. J Am Coll Radiol, 2021, 18(5): 713-729.
[9] 孙梦雅, 胡笑笑, 张繁,等. 卵巢-附件影像报告和数据系统(O-RADS)磁共振成像风险分层指南介绍和解读[J]. 影像诊断与介入放射学, 2022, 31(4): 243-251.
Sun MY, Hu XX, Zhang F, et al. Introduction and interpretation of ovarian-adnexal reporting and data system (O-RADS MRI)[J]. Diagn Imag & Intervent Radiol, 2022, 31(4): 243-251.
[10] Thomassin-Naggara I, Poncelet E, Jalaguier-Coudray A, et al. Ovarian-adnexal reporting data system magnetic resonance imaging (O-RADS MRI) score for risk stratification of sonographically indeterminate adnexal masses[J]. JAMA Netw Open, 2020, 3(1): e1919896.
[11] Patel-Lippmann KK, Sadowski EA, Robbins JB, et al. Comparison of International Ovarian Tumor Analysis Simple Rules to Society of Radiologists in Ultrasound Guidelines for Detection of Malignancy in Adnexal Cysts[J]. AJR Am J Roentgenol, 2020, 214(3): 694-700.
[12] Sadowski EA, Paroder V, Patel-Lippmann K, et al. Indeterminate adnexal cysts at US: prevalence and characteristics of ovarian cancer [J]. Radiology, 2018, 287(3): 1041-1049.
[13] Forstner R, Thomassin-Naggara I, Cunha TM, et al. ESUR recommendations for MR imaging of the sonographically indeterminate adnexal mass: an update [J]. Eur Radiol, 2017, 27(6): 2248-2257.
[14] Bernardin L, Dilks P, Liyanage S, et al. Effectiveness of semi-quantitative multiphase dynamic contrast-enhanced MRI as a predictor of malignancy in complex adnexal masses: radiological and pathological correlation[J]. Eur Radiol, 2012, 22(4): 880-890.
[15] Maturen KE, Blaty AD, Wasnik AP, et al. Risk stratification of adnexal cysts and cystic masses: clinical performance of society of radiologists in ultrasound guidelines[J]. Radiology, 2017, 285(2): 650-659.
[16] Sasaguri K, Yamaguchi K, Nakazono T, et al. External validation of ADNEX MR SCORING system: a single-centre retrospective study [J]. Clin Radiol, 2019, 74(2): 131-139.
[17] Pereira PN, Sarian LO, Yoshida A, et al. Accuracy of the ADNEX MR scoring system based on a simplified MRI protocol for the assessment of adnexal masses[J]. Diagn Interv Radiol, 2018, 24(2): 63-71.
[18] Ruiz M, Labauge P, Louboutin A, et al. External validation of the MR imaging scoring system for the management of adnexal masses[J]. Eur J Obstet Gynecol Reprod Biol, 2016, 205: 115-119.
[19] Sahin H, Panico C, Ursprung S, et al. Non-contrast MRI can accurately characterize adnexal masses: a retrospective study [J]. Eur Radiol, 2021, 31(9): 6962-6973.
[20] Taylor EC, Irshaid L, Mathur M. Multimodality imaging approach to ovarian neoplasms with pathologic correlation[J]. Radiographics, 2021, 41(1): 289-315.
[21] Thomassin-Naggara I, Belghitti M, Milon A, et al. O-RADS MRI score: analysis of misclassified cases in a prospective multicentric European cohort[J]. Eur Radiol, 2021, 31(12): 9588-9599.
[22] McDermott S, Oei TN, Iyer VR, et al. MR imaging of malignancies arising in endometriomas and extraovarian endometriosis[J]. Radiographics, 2012, 32(3): 845-863.
[23] Tanaka YO, Okada S, Yagi T, et al. MRI of endometriotic cysts in association with ovarian carcinoma[J]. AJR Am J Roentgenol, 2010, 194(2): 355-361.

(编辑　余　菁)